Computer-aided Diagnosis of Plus Disease in Retinal Fundus Images of Preterm Infants via Measurement of Vessel Tortuosity

Faraz Oloumi[1], Rangaraj M. Rangayyan[1*], and Anna L. Ells[1,2]

***Abstract*— An increase in retinal vessel tortuosity can be indicative of the presence of various diseases including retinopathy of prematurity (ROP). Accurate detection and measurement of such changes could help in computer-aided diagnosis of plus disease, which warrants treatment of ROP. We present image processing methods for detection and segmentation of retinal vessels, quantification of vessel tortuosity, and diagnostic-decision-making criteria that incorporate the clinical definition of plus-diagnosis. The obtained results using 110 retinal fundus images of preterm infants (91 without plus and 19 with plus) provide high sensitivity $= 0.89$ $(17/19)$ and excellent specificity $= 0.95$ $(86/91)$ in the diagnosis of plus disease.**

I. INTRODUCTION

Retinopathy of prematurity (ROP) is a retinal disease that manifests itself through changes to the vasculature [1]–[4]. Treatment of ROP is warranted based on the diagnosis of plus disease [1], which is defined by the presence of sufficient levels of increase in tortuosity and width of the retinal vessels. Plus disease is clinically diagnosed by visual and subjective comparison to a gold-standard image [1], [5].

Several measures of tortuosity have been proposed in the literature, which fall into two main categories: 1) length-to-chord (LTC) measures and 2) angle-based measures. Tortuosity measures are obtained using a skeletal representation of the vasculature derived using semiautomated image analysis algorithms or drafted manually.

The simplest definition of tortuosity is the LTC measure, which is the ratio of the true (geodesic) length of a segment to the length of the line connecting the segment's end points (chord) [2], [3], [6]. The LTC measure does not account for possible changes in the curvature of a segment; hence, an arched segment and a sinusoidal segment of the same true and chord lengths may lead to the same tortuosity value, which is undesirable. Some studies have proposed modified definitions of the LTC measure to overcome this limitation. Using curvature, Grisan et al. [7] separated vessel segments into curved and linear parts and then assigned each half of a given linear subsegment to its previous and next curved subsegments. Grisan et al. defined the tortuosity of the entire segment as the sum of the LTC of each subsegment normalized by the true length of the entire segment and weighted based on the number of subsegments (number of sign changes in the curvature). The proposed measure could provide misleading values if a subsegment does not contain any nonlinear parts.

The angle-based tortuosity measures are derived by defining a set of vectors of fixed length connecting various points on a given segment and using the angles formed at the tip and tail of two consecutively connected vectors to compute a tortuosity measure. Gelman et al. [6] defined tortuosity as the sum of all angles (SOA) between a set of vectors normalized by the total length of the segment. However, they did not specify the length of the vectors used to obtain the angles. Makkapati and Ravi [8] proposed a modified definition of the SOA measure by defining the angles using the two angular bisectors of three consecutively connected vectors normalized by the sum of the lengths of each subsegment. Lisowska et al. [9] used a similar approach as the SOA method; however, instead of defining an angle between successive vectors, the absolute change in the slope of the vectors was obtained and a measure of tortuosity was defined for a segment as the sum of the slope differences.

The tortuosity measures that use the SOA approach are dependent on the length of the vectors used on a segment to define the angles; short vectors may result in large angles, whereas long vectors may miss local variations. Obtaining an ideal representation of the center-lines of vessels is a difficult task that is prone to errors due to inaccuracies in detection, segmentation, and sampling; defining the orientation of a given vessel pixel using the coordinates of such a representation of vessels is also prone to errors.

In a preliminary study [10], we proposed a measure of tortuosity based on the orientation at each pixel of a vessel segment obtained during the vessel detection stage using Gabor filters. In this paper, we present comprehensive methods for computer-aided diagnosis (CAD) of plus disease using a large database of retinal fundus images of preterm infants. The methods include the use of Gabor filters for detection of vessels as well as obtaining the dominant orientation of vessels at each pixel, and morphological image processing methods to segment vessels and obtain their associated skeletal representation. Furthermore, statistical analysis of the variations in the orientation of vessels is used to detect linear segments and the measure of angle-variation-based tortuosity (AVT) is employed to determine abnormally tortuous vessels. Finally, clinically relevant diagnostic-decision-making procedures are used to diagnose plus disease.

II. MATERIALS AND METHODS

1) Database of Images: The proposed methods were tested with retinal fundus images from the Telemedicine for

[1]Department of Electrical and Computer Engineering, Schulich School of Engineering, University of Calgary, Calgary, AB, Canada, T2N 1N4. *ranga@ucalgary.ca.

[2]Division of Ophthalmology, Department of Surgery, Alberta Children's Hospital, Calgary, AB, Canada, T3B 6A8.

978-1-4244-9270-1/15/$31.00 ©2015 IEEE

ROP In Calgary (TROPIC) database [11]. The images of the TROPIC database were captured using the RetCam 130 camera [wide-field (130°)] and have a size of 640×480 pixels. The spatial resolution of the images is estimated to be 30 μm/pixel [12]. In total, 110 images from 41 patients, including 16 females and 25 males, were selected. Nineteen of the images are of patients diagnosed with plus disease and 91 show no signs of plus disease. At most, two images of the same patient were included for the same stage of ROP, with one image from each eye. Images of the same eye from the same patient were included in the test set only if the ROP stages were different at the time of imaging, as diagnosed by an expert pediatric ophthalmologist and retinal specialist (A. L. Ells). A training set of 10 images, including 5 without and 5 with plus disease were also selected. All abnormally tortuous vessel segments in the 5 training images with plus disease were manually identified by A. L. Ells. The images of the training set are independent of the test set. Images were not selected based on overall quality and/or vessel-to-background contrast. The project and protocol were approved by the Conjoint Health Research Ethics Board of the University of Calgary.

2) Segmentation of Vessel Skeleton: Gabor filters were implemented using the parameters τ, l, and K, representing average vessel thickness, vessel elongation, and total number of evenly spaced oriented filters over the range $[-\pi/2, \pi/2]$ [13]. The initial steps to obtain the skeleton image of vessels are: 1) Obtain the Gabor-magnitude and Gabor-angle-response images of the green-channel image [13]. 2) Normalize the Gabor-magnitude-response image. 3) Binarize the normalized Gabor-magnitude-response image using a threshold slider. 4) Remove 8-connected segments shorter than a maximum length (in pixels) as specified by the user. 5) Skeletonize the resulting binary image.

The threshold used to binarize the Gabor-magnitude-response image and the maxumum length of vessel segments to be removed were determined by the user. The previously marked center of the optic nerve head (ONH) was used to remove an elliptical area form the skeleton image, centered at the center of the ONH. The height and width of the ellipse were set based on the average ONH width (ONHW) and height in preterm infants [12]. Next, spurs 5 pixels or shorter in length were removed from the skeleton image, after which branching points on the skeleton were detected using morphological methods. An area of 3×3 pixels, centered at each branching point, was removed from the skeleton image to separate all vessel segments for further analysis. Morphological area open was used to remove segments of length less than 7 pixels.

3) Analysis of Variations in the Orientation of Vessel Segments: All disconnected vessel segments obtained in the previous step were detected and numbered. Each selected skeleton segment was analyzed in terms of its associated Gabor angle information to determine whether the segment contains linear subsegments. The first step to obtain linear subsegments of a selected vessel segment is to identify its pixels in the correct sequential order as follows: 1) Ensure that the current segment does not contain any branching points, i.e., it has exactly two end points. 2) Obtain the first end point of the segment. 3) Move sequentially along the skeleton segment one pixel at a time in a 3×3-pixel neighborhood centered at the previously selected pixel. 4) Store the sequential position of each traversed pixel in the segment as well as its associated Gabor-angle response in vectorial format. 5) Repeat steps $2-3$ until the second end point is reached.

In order to detect linear portions of the extracted skeleton segments, the statistical measure of median absolute deviation (MAD) [14] was obtained in a window of length 7 pixels applied to the sequenced Gabor-angle response, ϕ. Given a set of data points, P, MAD $= \text{median}\big[|P - \text{median}(P)|\big]$. A pixel on the same segment was marked as being linear only if all normalized MAD measures in a 7-pixel-long window centered at the current pixel are zero. A skeleton image of only linear segments was obtained using the normalized MAD measure. A skeleton image of nonlinear vessel segments was obtained by subtracting the image of linear segments from the original skeleton image. A local tortuosity index (LTI) was defined as $\text{LTI}(p) = \{|\sin[\phi(p) - \phi(p-1)]| + |\sin[\phi(p) - \phi(p+1)]|\}/2$, where p, $p-1$, and $p+1$ are the current, previous, and next pixels, respectively, along a nonlinear vessel segment. The measure of AVT was obtained over a nonlinear vessel subsegment as $\text{AVT} = \frac{1}{P}\sum_{p=1}^{P} \text{LTI}(p)$ [10], where P is the total number of pixels in the given subsegment.

The training set of images was used to compare the AVT measures for the abnormally tortuous and normal vessels, as marked by the retinal specialist, to obtain a suitable threshold. Based on this analysis, a threshold of $t = 0.07$ was determined. Each nonlinear vessel segment with AVT $> t$ was marked as being abnormally tortuous.

4) Diagnostic Decision Making: Clinical diagnosis of plus disease requires the presence of sufficient increase in tortuosity, as compared to the gold-standard image, in at least 2 quadrants of the image. Providing one average or overall measure of tortuosity for an image, or even for each quadrant of an image, may be misleading if the tortuous segments are not sufficiently long; two highly tortuous but short segments in two quadrants should not lead to a positive diagnosis. We propose diagnostic-decision-making procedures that follow the clinical definition of plus diagnosis as well as a minimum-length criterion. By analyzing the length of the abnormally tortuous vessels in the training set, as marked by the retinal specialist, a suitable minimum-length threshold for diagnosis of plus disease was obtained. To determine the total length of tortuous vessels in each quadrant, the skeleton image of the abnormally tortuous vessels was divided into 4 quadrants with reference to the center of the ONH. Every segment in each quadrant was then identified and its associated chain-code [15] representation was obtained. The length of each segment was computed as the number of even codes plus $\sqrt{2}$ multiplied by the number of odd codes multiplied by 30 μm.

A diagnosis of plus disease is made if an image contains at least $2.5\ mm$ of abnormally tortuous vessels in each of at least 2 quadrants or at least $5\ mm$ of abnormally tortuous vessels in any one quadrant. A second set of threshold values of $3\ mm$ or $6\ mm$ was also used to analyze the trade off between true-positive and true-negative rates.

III. RESULTS AND COMPARATIVE ANALYSIS

Values of $\tau = 7$ pixels, $l = 1$, and $K = 45$ were used to obtain the Gabor-magnitude and angle-response images. Fig. 1 illustrates the results of applying the proposed methods to an image from the TROPIC database that does not show any signs of plus disease. The total lengths of abnormally tortuous vessels were computed to be $0.93,\ 0,\ 0$, and $0.84\ mm$ in the four quadrants. Fig. 2 illustrates the same steps for an image with signs of plus disease. The total length of abnormally tortuous vessels in the four quadrants are $3.73,\ 6.56,\ 1.77$, and $7.84\ mm$.

Using the minimum-length thresholds of $2.5\ mm$ or $5\ mm$ of abnormally tortuous vessels, sensitivity and specificity of $0.89\ (17/19)$ and $0.95\ (86/91)$, respectively, were obtained. The thresholds of $3\ mm$ or $6\ mm$ provided sensitivity and specificity of $0.84\ (16/19)$ and $0.99\ (90/91)$, respectively.

To the best of our knowledge, only 4 studies have performed CAD of plus disease based on the quantification of vessel tortuosity and the use of a threshold for diagnosis. Studies conducted by Wallace et al. [2] and Heneghan et al. [3] used the LTC measure. Gelman et al. [16] and Koreen et al. [4] employed the LTC measure as well as the SOA approach [6] to quantify tortuosity. All of the mentioned studies have limited the area of analysis to a circle centered at the center of the ONH with radius $= 2\times$ONHW, used manual selection and/or correction of the vessel segments to be analyzed, and provided user-input parameters such as binarization threshold values and the location of the center of the ONH. Table I presents comparative analysis of the results of the mentioned studies.

The only study that is almost directly comparable to the present work was conducted by Wallace et al. [2]. Measures of LTC tortuosity from the gold-standard image (venules and arterioles combined) were obtained, and if an image had equal or greater tortuosity measures in at least two quadrants, the image was diagnosed as a case with plus disease.

Heneghan et al. [3] combined measurements from both arterioles and venules to obtain the average thickness and tortuosity values for an image. Using the combination of the two measures, Heneghan et al. obtained sensitivity $= 0.82$ and specificity $= 0.75$ in the diagnosis of threshold disease.

The studies conducted by Gelman et al. [16] and Koreen et al. [4] used the software package RISA [17]. In both studies, sensitivity and specificity values were determined by finding the intersection point between the sensitivity and specificity curves, plotted separately as functions of the ratio of the number of correctly identified vessels against the actual tortuosity measures. Such a measure does not classify the image, but classifies each single vessel. RISA requires the vessel segment under analysis to have at least one branching point. Manual correction of the detected branching points and manual input regarding whether the selected vessels are arterioles or venules, which were analyzed separately, were also required. Neither study provided diagnostic performance using venules and arterioles combined. Even though both the LTC and the SOA measures were employed in the mentioned studies, only the results obtained using the SOA measures are provided in Table I since the LTC measure performed poorly.

TABLE I

COMPARATIVE ANALYSIS BETWEEN THE PRESENT WORK AND SIMILAR STATE-OF-THE-ART STUDIES AVAILABLE IN THE LITERATURE. * VALUES OBTAINED USING VESSEL TORTUOSITY AND THICKNESS COMBINED. ** VALUES OBTAINED USING ONLY ARTERIOLE TORTUOSITY.

Study	# without/with plus disease	Sensitivity	Specificity
Heneghan et al. [3]	12/11	0.82^{*}	0.75^{*}
Gelman et al. [16]	21/13	0.76^{**}	0.76^{**}
Koreen et al. [4]	14/6	1.00^{**}	0.85^{**}
Wallace et al. [2]	11/5	0.82	0.80
Present work	91/19	0.89	0.95

IV. DISCUSSION

The proposed diagnostic-decision-making criteria combine the clinical definition of plus disease with practical understanding of a sufficiently tortuous vessel. The results indicate high performance in diagnosis of plus disease using a single feature with sensitivity $= 0.89$ and specificity $= 0.95$. As compared to the state-of-the-art methods for diagnosis of plus disease using tortuosity, our methods provide the highest specificity and only the sensitivity provided by Koreen et al. [4] using arteriole tortuosity is higher than that in the present work. Koreen et al. used only 6 images with plus disease and did not provide a performance measure using both arterioles and venules combined; a direct comparison between the results of the present study and the study of Koreen et al. may not be appropriate.

The proposed methods are fully automated, except for the binarization step, the initial removal of small segments, and marking of the center of the ONH. No single automated thresholding method provides consistent results for binarization of all images due to the variable nature of the retinal images of preterm infants, including varying pigmentation, blurring, and low vessel-to-background contrast. Combination of the results of multiple thresholding methods may lead to better binarization results [18]. The method of Rangayyan et al. [19] will be adapted in the future to detect automatically the center of the ONH.

All studies that have performed diagnosis of plus disease using tortuosity have provided a single measure of tortuosity for either each selected vessel segment [4], [6], [16], the entire image [3], or for each quadrant of the image [2]. However, since tortuosity is not formally defined, numerical representations of its quantitative measurement may not be meaningful to an ophthalmologist. Use of the AVT measure

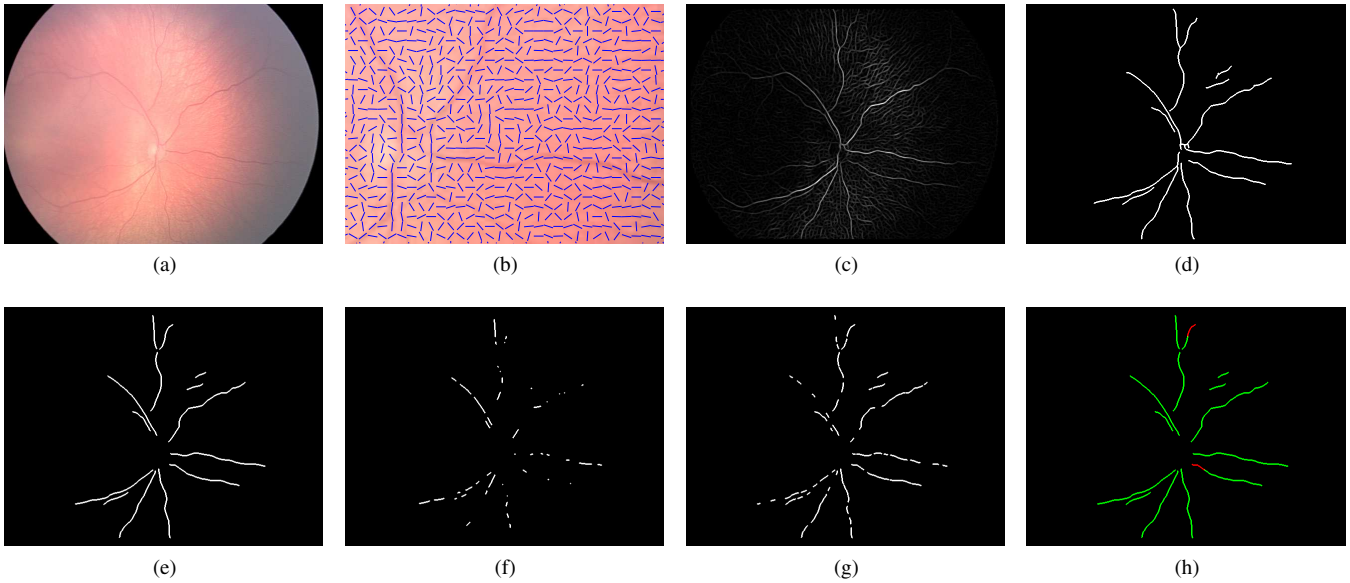

Fig. 1. a) Image 4002 showing no signs of plus disease. b) The Gabor-angle response for every fifth pixel for a portion of the image in part a). c) The Gabor-magnitude-response image obtained using the green-channel of the image in part a). d) The skeleton after thresholding the image in part c) at 0.125 of the normalized intensity and removal of 8-connected segments less than 70 pixels. e) The skeleton after removal of the ONH area and the branching points. f) The skeleton of the linear vessel segments obtained using the MAD measure. g) Skeleton image of the nonlinear vessel segments obtained by subtracting the image in part f) from the image in part e). h) Color-coded skeleton image distinguishing the abnormally tortuous vessel segments in red (threshold $= 0.07$) and the normal segments in green. Images in parts d-h) have been dilated using a disk of radius one pixel for better illustration.

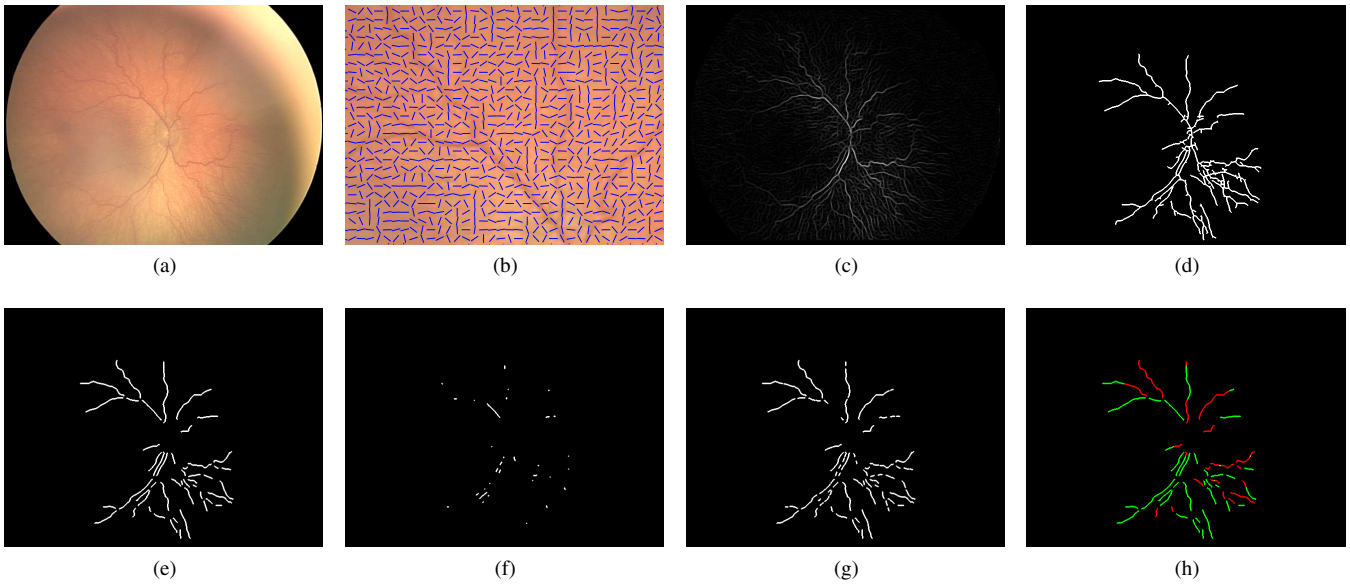

Fig. 2. a) Image 2203 that shows signs of plus disease. b-c) As in Fig. 1 b-c). d) The skeleton after thresholding the Gabor-magnitude-response image at 0.04 of the normalized intensity value and removal of 8-connected segments less than 100 pixels. e-h) As in Fig. 1 e-h).

to detect abnormally tortuous vessels and then to obtain the length of each of those vessels is more practical from a CAD point-of-view, and more meaningful to an ophthalmologist.

Even though the gold-standard image of plus disease has been used for clinical diagnosis, the image is believed to be atypical since it shows more vascular dilation and less tortuosity as compared to most cases with plus disease [20]. Secondly, the image possesses a narrow field of view, and does not reveal possible tortuous vessels in the periphery of the retina. All studies mentioned in Section III limited the area of analysis to the posterior of the retina. However, peripheral-vessel tortuosity has been shown to be more correlated to the presence of plus disease as compared to posterior-vessel tortuosity [21]. Given such limitations, it is beneficial to obtain any necessary thresholding parameters using an independent training set of images. In fact, based

on the results obtained in the present study, it is questionable whether posterior-arteriolar tortuosity is more important in diagnosis of plus disease than peripheral-venular tortuosity. The proposed methods are capable of detecting all tortuous vessels regardless of location.

All studies that have performed diagnosis of plus disease via quantification of vessel tortuosity have employed methods that involve manual marking of vessel segments, or manual selection and/or correction of parts of automatically detected vessels to include only the desired vessels for further analysis. The methods proposed in the present work are capable of distinguishing tortuous vessels in a given image without any manual selection and/or correction.

It would be of interest to combine the results of measurement of tortuosity with measurements of vessels thickness [22], as well as the openness of the major temporal arcade [23], to improve the diagnostic performance of plus diagnosis; this is a work in progress. Analysis of receiver operating characteristics needs to be performed to study the effects of the thresholds used on the final result.

V. CONCLUSION

In comparison to our pilot study [10], we observe that the use of the MAD measure to detect and remove linear parts of vessel segments improves the accuracy of the obtained tortuosity measures. The use of a training set to obtain thresholds for the AVT measure and to define the minimum-length criterion is advantageous and does not bias the final findings since the training and test sets are mutually independent.

The methods presented in this work are capable of distinguishing abnormally tortuous vessels and present high accuracy in diagnosis of plus disease and may be used for CAD in a clinical setting.

ACKNOWLEDGMENT

This work was supported by the Natural Sciences and Engineering Research Council of Canada. We thank Dr. Eliana Silva de Almeida for help with statistical analysis and April Ingram for help with the TROPIC database.

REFERENCES

[1] International Committee for the Classification of Retinopathy of Prematurity, "The international classification of retinopathy of prematurity revisited," *Archives of Ophthalmology*, vol. 123, pp. 991–999, 2005.

[2] D. K. Wallace, J. Jomier, S. R. Aylward, and M. B. Landers, III, "Computer-automated quantification of plus disease in retinopathy of prematurity," *Journal of American Association for Pediatric Ophthalmology and Strabismus*, vol. 7, pp. 126–130, April 2003.

[3] C. Heneghan, J. T. Flynn, M. O'Keefe, and M. Cahill, "Characterization of changes in blood vessels width and tortuosity in retinopathy of prematurity using image analysis," *Medical Image Analysis*, vol. 6, no. 1, pp. 407–429, 2002.

[4] S. Koreen, R. Gelman, M. E. Martínez-Pérez, L. Jiang, A. M. Berrocal, D. J. Hess, J. T. Flynn, and M. F. Chiang, "Evaluation of a computer-based system for plus disease diagnosis in retinopathy of prematurity," *Ophthalmology*, vol. 114, no. 12, pp. 59–67, 2007.

[5] M. F. Chiang, L. Jiang, R. Gelman, Y. E. Du, and J. T. Flynn, "Interexpert agreement of plus disease diagnosis in retinopathy of prematurity," *Archives of Ophthalmology*, vol. 125, no. 7, pp. 875–880, 2007.

[6] R. Gelman, M. E. Martínez-Pérez, D. K. Vanderveen, A. Moskowitz, and A. B. Fulton, "Diagnosis of plus disease in retinopathy of prematurity using retinal image multiscale analysis," *Investigative Ophthalmology & Visual Science*, vol. 46, no. 12, pp. 4734–4738, 2005.

[7] E. Grisan, M. Foracchia, and A. Ruggeri, "A novel method for the automatic grading of retinal vessel tortuosity," *IEEE Transactions on Medical Imaging*, vol. 27, no. 3, pp. 310–319, March 2008.

[8] V. V. Makkapati and V. V. C. Ravi, "Computation of tortuosity of two dimensional vessels," in *Eighth International Conference on Advances in Pattern Recognition (ICAPR)*, Kolkata, India, January 2015, pp. 1–4, IEEE.

[9] A. Lisowska, R. Annunziata, G. K. Loh, D. Karl, and E. Trucco, "An experimental assessment of five indices of retinal vessel tortuosity with the RET-TORT public dataset," in *36th Annual International Conference of the IEEE Engineering in Medicine and Biology Society (EMBC)*, Chicago, IL, August 2014, pp. 5414–5417.

[10] F. Oloumi, R. M. Rangayyan, and A. L. Ells, "Assessment of vessel tortuosity in retinal images of preterm infants," in *36th Annual International Conference of the IEEE Engineering in Medicine and Biology Society (EMBC)*, Chicago, IL, August 2014, pp. 5410–5413.

[11] P. L. Hildebrand, A. L. Ells, and A. D. Ingram, "The impact of telemedicine integration on resource use in the evaluation ROP ... analysis of the telemedicine for ROP in Calgary (TROPIC) database," *Investigative Ophthalmology & Visual Science*, vol. 50, pp. E–Abstract 3151, 2009.

[12] D. J. De Silva, K. D. Cocker, G. Lau, S. T. Clay, A. R. Fielder, and M. J. Moseley, "Optic disk size and optic disk-to-fovea distance in preterm and full-term infants," *Investigative Ophthalmology & Visual Science*, vol. 47, no. 11, pp. 4683–4686, 2006.

[13] R. M. Rangayyan, F. J. Ayres, Faraz Oloumi, Foad Oloumi, and P. Eshghzadeh-Zanjani, "Detection of blood vessels in the retina with multiscale Gabor filters," *Journal of Electronic Imaging*, vol. 17, pp. 023018:1–7, April-June 2008.

[14] T. Pham-Gia and T.L. Hung, "The mean and median absolute deviations," *Mathematical and Computer Modelling*, vol. 34, no. 7-8, pp. 921 – 936, 2001.

[15] H. Freeman, "On the encoding of arbitrary geometric configurations," *Electronic Computers, IRE Transactions on*, vol. EC-10, no. 2, pp. 260–268, June 1961.

[16] R. Gelman, L. Jiang, Y. E. Du, M. E. Martínez-Pérez, J. T. Flynn, and M. F. Chiang, "Plus disease in retinopathy of prematurity: Pilot study of computer-based and expert diagnosis," *Journal of American Association for Pediatric Ophthalmology and Strabismus*, vol. 11, no. 6, pp. 532–540, 2007.

[17] M. E. Martínez-Pérez, A. D. Hughes, A. V. Stanton, S. A. Thom, N. Chapman, A. A. Bharath, and K. H. Parker, "Retinal vascular tree morphology: A semi-automatic quantification," *IEEE Transactions on Biomedical Engineering*, vol. 49, no. 8, pp. 912–917, 2002.

[18] R. Medina-Carnicer, A. Carmona-Poyato, R. Mu noz Salinas, and F. J. Madrid-Cuevas, "Determining hysteresis thresholds for edge detection by combining the advantages and disadvantages of thresholding methods," *IEEE Transactions on Image Processing*, vol. 19, no. 1, pp. 165–173, January 2010.

[19] R. M. Rangayyan, X. Zhu, F. J. Ayres, and A. L. Ells, "Detection of the optic nerve head in fundus images of the retina with Gabor filters and phase portrait analysis," *Journal of Digital Imaging*, vol. 23, no. 4, pp. 438–453, August 2010.

[20] B. V. Davitt and D. K. Wallace, "Plus disease," *Survey of Ophthalmology*, vol. 54, no. 6, pp. 663–670, Nov-Dec 2009.

[21] K. M. Keck, J. Kalpathy-Cramer, E. Ataer-Cansizoglu, S. You, D. Erdogmus, and M. F. Chiang, "Plus disease diagnosis in retinopathy of prematurity: Vascular tortuosity as a function of distance from optic disk," *Retina*, vol. 33, no. 8, pp. 1700–1707, 2013.

[22] F. Oloumi, R. M. Rangayyan, and A. L. Ells, "Measurement of vessel width in retinal fundus images of preterm infants with plus disease," in *Proc. 2014 IEEE International Symposium on Medical Measurements and Applications (MeMeA)*, Lisbon, Portugal, June 2014, pp. 1–5.

[23] F. Oloumi, R. M. Rangayyan, and A. L. Ells, "Quantification of the changes in the openness of the major temporal arcade in retinal fundus images of preterm infants with plus disease," *Investigative Ophthalmology & Visual Science*, vol. 55, no. 10, pp. 6728–6735, October 2014.